

Conversion of *n*-pentane and of *n*-butane catalyzed by platinum-containing WO_x/TiO₂

S. Eibl,^a R. E. Jentoft,^b B. C. Gates^{ab} and H. Knözinger^a

^a Institut für Physikalische Chemie, LMU München, Butenandtstrasse 5-13 (Haus E), 81377, München, Germany

^b Department of Chemical Engineering and Materials Science, University of California, Davis, CA 95616, USA

Received 5th January 2000, Accepted 6th April 2000

Published on the Web 11th May 2000

Tungstated titania, with and without platinum, was used to catalyze the conversion of *n*-butane and of *n*-pentane at atmospheric pressure and temperatures in the range of 423–573 K, both in the presence and in the absence of H₂ in the feed stream to a flow reactor. The catalysts were active for isomerization and cracking, and the products included alkenes, in contrast to those observed in catalysis by tungstated zirconia. The catalytic activity of tungstated titania is much less than that of sulfated zirconia and similar to that of tungstated zirconia. The results characterizing tungstated titania indicate a bifunctional reaction network involving metal and acidic sites responsible for hydrogenation/dehydrogenation and carbenium ion reactions, respectively. Platinum in the catalyst and H₂ in the feed strongly suppress the otherwise rapid catalyst deactivation associated with coke deposition. The catalyst was found to be stable after a period of initial deactivation, and kinetics data are reported for partially deactivated catalysts. High platinum contents lead to high selectivities for cracking in the presence of H₂ and high selectivities for unsaturated products in the absence of H₂. Increasing tungsten loadings raise catalyst acidity and favor isomerization. The performance of tungstated titania containing platinum resembles that of the zirconia-based catalysts less than it resembles the performance of platinum supported on (chlorided) alumina, a well-known naphtha reforming catalyst.

Introduction

Branched alkanes are clean-burning automotive fuel components with high octane numbers. They are favored thermodynamically over straight-chain alkanes at low temperatures, and consequently processes for isomerization of straight-chain alkanes benefit from highly active catalysts that allow operation at low temperatures. Most such catalysts used currently are either (a) strongly acidic halides, which are corrosive and difficult to dispose of safely, and which also catalyze cracking, and (b) metal-containing zeolites, which are bifunctional (operating in the presence of H₂) and require high temperatures because their activities are relatively low. Alternatively, catalysts such as (promoted) sulfated zirconia are beginning to find applications as alkane isomerization catalysts,¹ being highly active, noncorrosive, and easy to dispose of properly. However, these nonhalide solid acids undergo rapid deactivation,² in part by coke formation and possibly by loss of sulfur.³ Tungstated zirconia offers an alternative of less active but more stable catalysts than sulfated zirconia. Promotion of the sulfated and tungstated catalysts with platinum increases activity and selectivity for isomerization and suppresses deactivation;^{4–6} H₂ in the feed prolongs catalyst life.⁷

Oxides that can be sulfated to give catalysts with high activities for alkane isomerization include, besides zirconia, titania and iron oxide.⁸ Consequently, one might expect that tungstated oxides other than zirconia would be of interest as alkane isomerization catalysts. For example, tungstated titania catalysts have been found to exhibit *n*-pentane isomerization activity,⁹ but the activity is low, and no further investigations have been reported. Our goal was to prepare and characterize platinum-promoted tungstated titania and to

compare its catalytic performance for conversion of *n*-pentane and of *n*-butane with that of promoted tungstated zirconia.

Experimental methods

Catalyst preparation

Tungstated titania catalysts were prepared by suspension of hydrous titanium oxide [precipitated from titanium isopropoxide (Heraeus, 99%) by the addition of water] in aqueous solutions containing amounts of ammonium metatungstate (Fluka, >85% WO₃) sufficient to yield calcined materials with loadings between 10 and 20 wt.% WO₃. Water was removed from the suspensions by evaporation, and the samples were dried at 383 K for 12 h and calcined at 923 K for 2 h in stagnant air. Platinum was subsequently added by the incipient wetness method with aqueous solutions of Pt(NH₃)₄(NO₃)₂ (Fluka, >99.9%), and the samples were calcined at 723 K for 2 h and reduced *in situ* in flowing H₂ [20 ml(NTP) min⁻¹] at 523 K. The samples contained 0.3 to 3 wt.% Pt. The sample nomenclature is as follows: the supported catalysts are referred to as Pt_xW_y, where *x* is the wt.% Pt and *y* the wt.% WO₃, with the remainder being TiO₂.

A tungstated zirconia catalyst containing 19 wt.% WO₃ and 0.3 wt.% Pt was prepared analogously by impregnation of hydrous zirconium oxide (MEL Chemicals), as described previously.¹⁰

Surface area measurements

The BET surface areas of the catalysts were measured with a Sorptomatic 1800 instrument (Carlo Erba) after the samples had been dried at 473 K in dynamic vacuum for 1 h.

Temperature-programmed reduction

Temperature-programmed reduction (TPR) was carried out with a mixture of 5 vol.% H₂ in N₂ at a flow rate of 12 ml min⁻¹. The temperature was ramped from 298 to 1073 K at 10 K min⁻¹; the catalyst sample mass was 0.250 g. Hydrogen consumption was measured with a thermal conductivity (TC) detector.

Platinum dispersion

Platinum dispersions ($Pt_{\text{surface}}/Pt_{\text{total}}$) were measured with a pulse flow method whereby pulses of CO (75 μl) were injected into a H₂ stream [25 ml(NTP) min⁻¹] and passed through a bed containing 0.250 g of catalyst particles. CO adsorption on the platinum surface was measured by monitoring the CO concentration leaving the bed with a TC detector. Subsequent pulses were injected until the amount of CO taken up reached zero. Dispersions were calculated by integration of the amount of CO taken up.

Low-temperature infrared spectroscopy with adsorbed CO

Infrared spectra were recorded with a Bruker IFS-66 FTIR spectrometer equipped with a liquid N₂-cooled MCT detector. Self-supporting wafers of catalyst (*ca.* 15–20 mg cm⁻²) were pressed at *ca.* 20 000 kPa and pretreated in dry O₂ [50 ml(NTP)/min⁻¹] at 673 K for 1 h and reduced in dry H₂ for 2 h at 523 K. The pretreated samples were cooled to liquid N₂ temperature under vacuum (<10⁻⁴ kPa) and exposed to CO at increasing equilibrium pressures in the range of 0.01–4 kPa. The cell is described elsewhere.¹¹

Catalysis experiments

Before each catalysis experiment, the catalyst in a stainless-steel flow microreactor¹² was heated in dry air [20 ml(NTP) min⁻¹; heating rate 10 K min⁻¹] to 673 K and held at 673 K for 1 h followed by reduction in H₂ [20 ml(NTP) min⁻¹] at 523 K for 1 h. The catalyst particles (0.20 to 0.50 g) were mixed with inert $\alpha\text{-Al}_2\text{O}_3$ particles to give a mass of particles of 1.5 g. Reactions of *n*-pentane or of *n*-butane were conducted at 101 kPa in the temperature-controlled microreactor. The alkane was mixed with N₂ (Puritan Bennett) and sometimes also with H₂ (99.999%, generated by electrolysis of water in a Balston hydrogen generator). The partial pressure of *n*-pentane or of *n*-butane in the reactant stream was varied from 0.17 to 1.0 kPa. The space velocity (WHSV) was varied from 0.036 to 0.440 g of alkane/(g of catalyst \times h). The reactor feed, for example, was 1 vol.% alkane in N₂ [20 ml(NTP) min⁻¹] or 1 : 1 mixtures by volume of H₂ and 1 vol.% alkane in N₂ [40 ml min⁻¹]. Products were analyzed by on-line gas chromatography (Hewlett Packard 5890) using a 0.52 mm \times 30 m alumina PLOT column.

Results

Catalyst surface areas

The samples had BET surface areas in the range of 65 to 80 m² g⁻¹, with slightly higher values for higher tungsten loadings.

Platinum dispersions

Calculation of the dispersion from CO uptake data collected using the pulse flow method requires the assumption of an adsorption stoichiometry. The stoichiometry assumed for our calculations was 1 : 1 CO : Pt; however, the adsorption of bridge-bonded CO, which has been observed by infrared spectroscopy (*vide infra*) in those samples with high platinum loadings (Pt₁W_y, Pt₃W_y) causes the adsorption to be characterized

by a lower CO : Pt ratio. Therefore, the data representing adsorption of CO on catalysts with high platinum contents are expected to result in too-high dispersion values. It is recognized that the pulse flow method is limited in its ability to give a quantitative measure of the dispersion; however, the technique is useful for the identification of correlations between catalyst properties and platinum surface area. The results (Table 1) indicate that high platinum or tungsten contents correspond to low platinum dispersions. At high tungsten loadings, exceeding those sufficient for monolayer coverage of the support (*ca.* 10% WO₃),¹³ we infer that the tungsten oxide phase was sufficient to cover a substantial part of the platinum. Thus, the relatively low platinum dispersions indicated by the data for the samples with high tungsten loadings are not likely to be an indication of relatively large (low-area) platinum particles, but instead to be an indication of a limitation of the method for determining true dispersions of platinum in such samples.

Temperature-programmed reduction

The reduction profiles representing the uncalcined platinum-containing samples treated in flowing H₂ (Fig. 1, curves b, d, and e) show intense signals in the range of 400–600 K. These signals were not observed for the platinum-free samples (Fig. 1, curves a and c), and they are therefore attributed to reduction of Pt²⁺ to Pt⁰. Weak reduction signals at 640–740 K with H₂ consumptions corresponding to 0.2 electrons per W atom have been reported for WO_x/ZrO₂.^{14,15} Similarly, for our samples, this first reduction step of tungsten (with a formal stoichiometry of WO₃ \rightarrow WO_{2.9}) is followed by a reduction to WO₂, with signals observed at temperatures above 900 K (Fig. 1, curve c); a further reduction to W⁰, which is not depicted in Fig. 1, occurs only at temperatures above 1200 K.

The addition of platinum to the catalysts led to shifts in the tungsten reduction signals to lower temperatures, by about 100 K for Pt_{0.3}W₁₀ and by about 50 K for Pt_{0.3}W₂₀, relative to the values for the platinum-free samples with the same tungsten contents.

Acid site characterization

The results of acid site characterization of several samples by low-temperature infrared spectroscopy of adsorbed CO are presented in Fig. 2. The spectra show bands at 2143 cm⁻¹, characteristic of physisorbed CO, as well as at 2170 cm⁻¹, indicative of CO adsorbed on Brønsted acid sites. Samples Pt_xW₁₀ and Pt_xW₂₀ show bands at 2194 and 2201 cm⁻¹, respectively, which are indicative of CO on Lewis acid sites. Bands characterizing samples W₁₀, W₁₅, and W₂₀ at 2194,

Table 1 Platinum dispersions in catalyst samples with various tungsten and platinum contents^a

Catalyst composition (wt.%)		Platinum dispersion (%)
Pt	WO ₃	
0.3 ^b	10	10
0.3 ^b	15	15
0.3 ^b	20	15
3 ^b	10	17
3 ^b	15	12
3 ^b	20	11
3 ^c	10	13
3 ^c	15	3
3 ^c	20	3

^a Samples were calcined at 923 K before the addition of platinum and at 723 K after the addition of platinum. ^b Reduced at 473 K.

^c Reduced at 1073 K.



Fig. 1 Temperature-programmed reduction profiles: (a) W_{10} ; (b) $Pt_{0.3}W_{10}$; (c) W_{20} ; (d): $Pt_{0.3}W_{20}$; (e) Pt_3W_{20} (spectra normalized and adjusted vertically).

2200, and 2206 cm^{-1} (not shown), respectively, show an increasing energy with increasing tungsten content. These bands at *ca.* 2200 cm^{-1} are attributed to Lewis acid sites with strongly overlapping bands for CO on Ti^{4+} and W^{6+} sites.

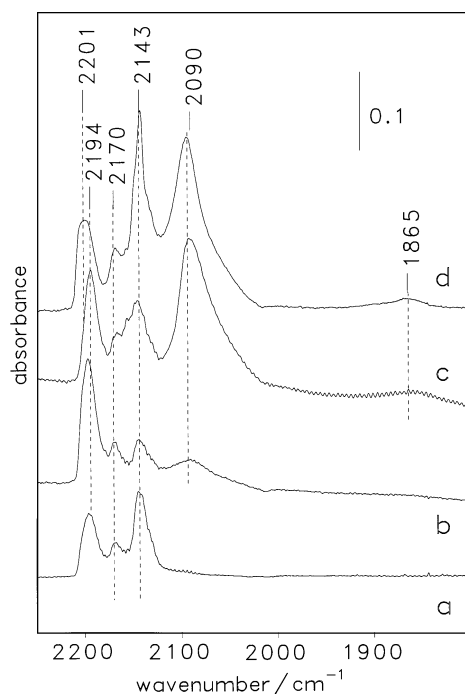


Fig. 2 Low-temperature (88 K) infrared spectra of catalysts in the presence of 4 kPa of CO: (a) W_{10} ; (b) $Pt_{0.3}W_{10}$; (c) Pt_3W_{10} ; (d) Pt_3W_{20} .

The Lewis acid strengths are slightly less (CO vibration frequency about 5 cm^{-1} lower) for samples with high tungsten and platinum loadings than for the platinum-free samples. The bands at 2090 and 1865 cm^{-1} are attributed to CO adsorbed on platinum in linear and bridged configurations, respectively.¹⁶ Band positions and intensities of CO on Brønsted acid sites are indistinguishable from each other in the spectra representing the platinum-free and platinum-containing catalysts. Shifts in the OH bands characterizing platinum-free samples (at approximately 3660 cm^{-1}) induced by CO adsorption were found to be 215, 230, and 240 cm^{-1} for W_{10} , W_{15} , and W_{20} (not shown), respectively. OH stretching bands were not detected in the black platinum-containing samples because of low signal-to-noise ratios at frequencies > 3500 cm^{-1} ; however, the addition of platinum to the WO_3/TiO_2 samples is not expected to have had a strong influence on the Brønsted acidity.¹⁷ The data indicate strong Brønsted acid sites¹⁸ that increase in strength with increasing tungsten content.

Performance of catalysts without platinum

Catalysts without platinum and with a tungsten loading (about 25% WO_3) that was found to give nearly the maximum activity catalyzed the conversion of *n*-pentane to give yields, defined as $100 \times (\text{concentration of product in the effluent stream}) / (\text{concentration of alkane in the feed})$, of about 1.2%, with selectivities for isopentane, defined as $(\text{concentration of isopentane in the effluent stream}) / (\text{total product concentration in the effluent stream})$, of about 85% for a feed of 1% *n*-pentane in 1 : 1 H_2/N_2 at 573 K. The yields were initially relatively high at a WHSV of 0.072 g of alkane/(g of catalyst \times h) and declined rapidly, becoming nearly constant at about 0.6% after several hours on stream. As the temperature was raised, the initial conversion of *n*-pentane increased from 1.2% at 573 K to 6.0% at 698 K. This increase in conversion was accompanied by a decrease in selectivity for the isomerization product (isopentane), from 85% at 573 K to 24.4% at 698 K, and an increase in the selectivity for cracking products (particularly methane), from 15% at 573 K to 75.6% at 698 K. Without H_2 in the feed there was no measurable conversion of a feed of 1% *n*-pentane in N_2 [20 ml min^{-1}] at temperatures up to 673 K with 0.5 g of WO_3/TiO_2 in the reactor. Further results are presented in a thesis.¹⁷

Performance of platinum-containing catalysts

***n*-Pentane and *n*-butane feeds without H_2 .** At 523 K the major product of reaction of *n*-pentane was initially the isomerization product isopentane, with smaller amounts of the cracking products isobutane, *n*-butane, and C_1 – C_3 alkanes. At a WHSV of 0.18 g of alkane/(g of catalyst \times h), these saturated products are characterized by initially high yields (*e.g.*, *ca.* 50% to isopentane) at 5 min on stream followed by rapid catalyst deactivation within the first 2 h on stream. In addition to saturated products, there were significant amounts of several C_5 alkenes, which were characterized by initially low yields followed by increasing yields to maxima of about 3.1 to 4.4% at 1 to 4 h on stream, followed by gradually decreasing yields of these products. Traces of C_6 and higher hydrocarbons were also present in the product stream (Table 2).

When the reactant was *n*-butane, the major product at 523 K was initially isobutane, with smaller amounts of C_1 – C_3 alkanes (Fig. 3). At a WHSV of 0.14 g of alkane/(g of catalyst \times h) these saturated products were characterized by initially high yields (*e.g.*, *ca.* 12% to isobutane) at 5 min on stream followed by rapid deactivation within the first 2 h on stream. In addition to these saturated products there were significant amounts of butenes, including *trans*-but-2-ene, *cis*-but-2-ene, but-1-ene, and isobutylene, which were characterized by initially low yields followed by increasing

Table 2 Catalyst performance data characterizing conversion of *n*-pentane (at 523 K) and of *n*-butane (at 573 K)^a

Reactant	Catalyst composition (wt.%)		TOS _{1/2} /h	Maximum yield (%)				Approx. carbon loss to catalyst (%)
	Pt	WO ₃		At TOS = 5 min		At TOS ≈ 1–4 h		
				Isopentane	C ₁ –C ₄	Pentenes	C ₆₊	
<i>n</i> -pentane	0.3	10	0.22	22	2.7	3.1(after ~1.0 h)	3.1	12
	0.3	20	0.28	17	3.1	2.2(after ~1.8 h)	2.2	25
	1	20	0.35	51	6.3	4.2(after ~2.5 h)	4.2	12
	3	20	0.56	60	4.9	4.4(after ~3.7 h)	4.5	11
<i>n</i> -butane	0.3	20	0.19	12	10.0	8.1(after ~2.6 h)	4.3	
	3	20	0.20	21	14.2	12.0(after ~2.8 h)	2.8	

^a The feed partial pressures were the following: alkane, 1 kPa; N₂, 100 kPa; the feed flow rate was 20 ml(NTP) min⁻¹; and the catalyst mass was 0.5 g.

values to maximum total yields of unsaturated products of about 10% at 2 to 5 h on stream followed by gradually decreasing yields of these products (Table 2). Thus, the occurrence of isomerization and of cracking is common to *n*-pentane and *n*-butane.

The yield of isobutylene from *n*-butane passed through a maximum with time on stream (Fig. 3). Thus, an induction period is evident, and it is similar to the induction periods representing the other butenes. The decline in yield of isobutylene following the induction period parallels the decline in yield of isobutane. Similar statements pertain to *n*-pentane conversion, but we were not able to distinguish between at least four of the unsaturated C₅ compounds. Thus, for each reactant, *n*-pentane and *n*-butane, we infer that the yield of the isoalkene proceeds *via* a combination of reactions rather than

a single reaction. The formation of alkenes shows that the catalyst is a dehydrogenation catalyst. The decrease in yield of branched products with time on stream (TOS) suggests a decreasing isomerization activity of the catalyst with TOS.

A carbon balance on the reactant and product streams (Table 2) shows an initially high and rapidly decreasing loss of carbon from the reactant stream to the catalyst. Thus, the catalyst deactivation is attributed (at least in part) to coke formation; coke formation is also an indication of the dehydrogenation activity of the catalyst. The profile of carbon loss with TOS is similar in shape to the profile of yield of isopentane from *n*-pentane (or of isobutane from *n*-butane) with TOS, in contrast to the profiles of yields of alkenes from alkanes with TOS.

***n*-Pentane feeds without H₂: effect of temperature.** In the *n*-pentane isomerization catalyzed by Pt/WO₃/TiO₂, the temperature influenced the conversion, selectivity, and rate of catalyst deactivation. To quantify the rate of deactivation, we use the parameter time on stream corresponding to a conversion equal to half of the initial conversion (TOS_{1/2}). The reported values of TOS_{1/2} were found by extrapolation of the conversion data to zero TOS and interpolation to half of the initial value by using an exponential fit to the conversion *vs.* TOS data.¹⁹

The trends in the yields of different products formed from *n*-pentane in the temperature range of 423–598 K at 5 min TOS are as follows: Higher temperatures gave higher yields of C₁–C₄ saturated products and isobutane. With increasing temperature, the yield of isopentane passed through a maximum at 523 K (Table 3). The trends in the selectivities for C₁–C₄ saturated products and isobutane parallel those rep-

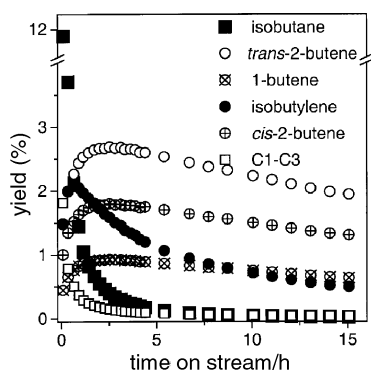


Fig. 3 Conversion of *n*-butane in a flow reactor containing Pt_{0.3}W₂₀ catalyst. Feed, *n*-butane (1 kPa) in N₂ (100 kPa); temperature, 573 K.

Table 3 Yields, selectivities, times on stream for half conversions (TOS_{1/2}) and carbon losses for TOS = 5 min in *n*-pentane conversion catalyzed by Pt₁W₂₀^a

Reaction temp./K	TOS _{1/2} /h	Yield and selectivity (%)										Approx. carbon loss to catalyst %
		At TOS = 5 min						At TOS = 2 h				
		C ₁ –C ₄ sat. ^b		Isobutane		Isopentane		C ₅ unsat. ^c		C ₆₊		
		Yield	Sel.	Yield	Sel.	Yield	Sel.	Yield	Sel.	Yield	Sel.	
423	0.98	0.05	0.5	0.2	1.5	11.2	98.1	0.13	21.0	0.43	1.3	0
523	0.41	1.71	2.96	5.5	7.41	51.1	84.2	4.39	96.7	2.30	0.9	12
598	0.35	16.6	24.5	12.5	19.3	32.0	49.2	18.24	89.5	3.70	1.8	25

^a The feed partial pressures were the following: *n*-pentane, 1 kPa; N₂, 100 kPa; the feed flow rate was 20 ml(NTP) min⁻¹; the catalyst mass was 0.5 g. ^b Saturated. ^c Unsaturated.

representing the yields of these products, with the selectivities increasing with increasing temperature. In contrast, selectivity for isopentane decreased with increasing temperature.

Increasing the temperature led to increasing production of unsaturated and oligomerized compounds, which likely include coke precursors. The increasing loss of carbon from the gas stream to the catalyst with increasing temperature is consistent with the observed deactivation and the formation of coke on the catalyst surface.

At 598 K, initial yields of isomerization products are expected to have been higher than those at lower temperatures (Table 3), but the opposite is apparently indicated by the data at TOS = 5 min. The apparent anomaly is explained by rapid deactivation during the first 5 min on stream and conversion of the *n*-pentane to secondary products after 5 min TOS. At this relatively high temperature, we were unable to extrapolate the data to measure the initial yield accurately.

***n*-Pentane and *n*-butane feeds without H₂: effects of platinum and WO₃ contents.** In the conversion of *n*-pentane at 523 K, increasing the catalyst platinum loading from 0.3 to 3.0% increased the yield of isopentane and retarded the deactivation for conversion to isopentane (TOS_{1/2} increased from 0.28 to 0.56 h). In contrast, increasing the tungsten content of a catalyst containing 0.3% Pt from 10 to 20% WO₃ led to only a slight decrease in the yield of isopentane and a slight increase in TOS_{1/2} (Table 2). In the isomerization of *n*-butane at 573 K, a higher platinum content (3% vs. 0.3%) in a 20% WO₃ catalyst led to increases in both the yield of isobutane and the yield of C₁–C₃ products (Table 2). A carbon balance on the reactant and product streams showed essentially no dependence on the platinum or tungsten content of the catalyst.

***n*-Pentane and *n*-butane feeds with H₂.** When *n*-pentane in a 1 : 1 mixture of H₂ and N₂ was fed to a reactor containing a Pt_{0.3}W₂₀ catalyst at 523 K, the major product was initially propane, with lesser amounts of isopentane, *n*-butane, ethane, and methane (Fig. 4). The yields of the cracking products decreased substantially during the first 4 h on stream, whereas the yield of isopentane underwent a brief induction period during the first hour on stream. Yields of both isomerization and cracking products became nearly stable after 6 h on stream and to the end of the run (up to 12 h on stream).

When *n*-butane in a 1 : 1 mixture of H₂ and N₂ was fed to a reactor containing Pt_{0.3}W₂₀ catalyst at 573 K, the major

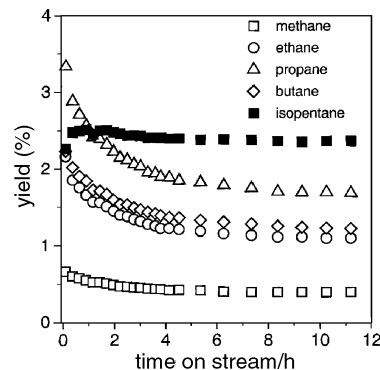


Fig. 4 Conversion of *n*-pentane in a flow reactor containing Pt_{0.3}W₂₀ catalyst. Feed, *n*-pentane (1 kPa) with H₂ (50 kPa) in N₂ (50 kPa); temperature, 523 K.

product was propane, with lesser amounts of methane, ethane, and isobutane. The H₂ markedly reduced the rate of catalyst deactivation. In contrast to the reaction carried out with platinum-containing catalysts without H₂, when H₂ was present in the feed there was no measurable loss of carbon to the catalyst.

***n*-Pentane and *n*-butane feeds with H₂: effects of platinum and WO₃ contents.** The selectivities for the reactions of *n*-pentane and of *n*-butane, at 523 and 573 K, respectively, are presented in Table 4. In the conversion of *n*-pentane at a WHSV of 0.18 g of alkane/(g of catalyst × h), catalysts containing low loadings of platinum (0.3% Pt) with 10 to 20% WO₃ gave conversions less than 7%, with nearly equimolar amounts of ethane and propane, on the one hand, and of methane and *n*-butane, on the other. Increasing the WO₃ contents of these samples led to increased yields of the isomerization product, isopentane, and to slight decreases in the yields of cracking products (C₁–C₄ alkanes). Catalysts with higher platinum loadings (3 wt.%) containing 20% WO₃ gave conversions up to 38% and higher selectivities for methane than for *n*-butane and higher selectivities for ethane than for propane (Table 4). Increasing the platinum loading in these samples reduced the selectivity for isopentane. The Pt_{0.3}W₂₀ sample is characterized by the highest selectivity for isopentane and the Pt₁W₂₀ sample by the highest yield of isopentane.

The trends for *n*-butane conversions at 573 K are similar to those for *n*-pentane conversion at 523 K. Higher tungsten

Table 4 Yields in conversion of *n*-pentane (at 523 K) and of *n*-butane (at 573 K) and selectivities [normalized (norm.) and molar, see text] after 12 h on stream^a

Reactant	Catalyst composition (wt%)		Yield (%)		Selectivity (%)											
	Pt	WO ₃	C ₁ –C ₄	Isopentane	Methane		Ethane		Propane		Isobutane		<i>n</i> -Butane		Isopentane	
					Norm.	Molar	Norm.	Molar	Norm.	Molar	Norm.	Molar	Norm.	Molar	Norm.	Molar
<i>n</i> -pentane	0.3	10	4.9	0.57	8.4	21.4	22.4	28.7	33.6	28.7	0.2	0.1	24.9	15.9	10.5	5.3
	0.3	15	4.5	0.87	7.4	19.6	20.9	27.8	31.8	28.2	0.2	0.1	23.5	15.6	16.3	8.7
	0.3	20	4.3	2.34	5.6	17.1	16.0	23.4	24.6	23.9	0.3	0.3	18.2	13.8	35.2	21.5
	1	20	12.0	4.49	7.8	20.9	21.6	29.0	27.3	24.5	0.4	0.3	15.6	10.6	27.3	14.8
	3	20	35.2	2.74	11.3	26.1	29.3	33.8	35.3	27.1	0.4	0.2	16.5	9.5	7.2	3.3
<i>n</i> -butane	0.3	10	11.9	0.35	Methane		Ethane		Propane		Isobutane					
					Norm.	Molar	Norm.	Molar	Norm.	Molar	Norm.	Molar				
	0.3	20	6.8	0.52	Methane		Ethane		Propane		Isobutane					
					Norm.	Molar	Norm.	Molar	Norm.	Molar	Norm.	Molar				
	3	20	97.5	0.65	Methane		Ethane		Propane		Isobutane					
Norm.					Molar	Norm.	Molar	Norm.	Molar	Norm.	Molar					

^a The partial pressures: alkane, 1 kPa; H₂, 50 kPa; N₂, 50 kPa; feed flow rate, 40 ml(NTP) min⁻¹; catalyst mass, 0.25 g.

loadings gave increased yield of (and selectivities for) the isomerization product, isobutane. Increasing platinum content resulted in increased yields of cracking products (methane, ethane, and propane) and decreased selectivity for isobutane.

***n*-Pentane and *n*-butane feeds with H₂: effect of space velocity** There was no significant effect on selectivity of variation of the space velocity from 0.036 to 0.440 g of alkane/(g of catalyst × h) for catalysts containing 0.3 wt.% Pt. However, there was a significant effect when the catalysts contained more than 0.3 wt.% Pt (Pt₁W₂₀ and Pt₃W₂₀). In the conversion of *n*-pentane in the presence of Pt₃W₂₀ at 473 K, the selectivity for the isomerization product (isopentane) increased with increasing space velocity, and the selectivity for the cracking products (methane, ethane, propane, and butane) decreased.

Measurements after 15 h on stream are characterized by stable, nearly constant conversions (at values lower than the maximum) and linear correlations of conversions with inverse space velocity w/F (catalyst mass/alkane molar flow rate) (Fig. 5). The slopes of the straight lines fitting the data were used to calculate reaction rates (Table 5). The calculated rates under steady-state conditions represent isomerization and cracking reactions.

***n*-Pentane and *n*-butane feeds with H₂: effect of temperature.** The catalyst samples containing 0.3% Pt reached nearly steady-state conversion when run for 12 h on stream, *i.e.*, the rate of deactivation became almost negligible after this period at temperatures up to 623 K. Thus, these partially deactivated and nearly stable catalysts presented the opportunity for measurement of the temperature dependence of the rates of the catalytic reactions.

Isomerization selectivity and yield increased with increasing temperature in the range of 473 to 623 K for samples

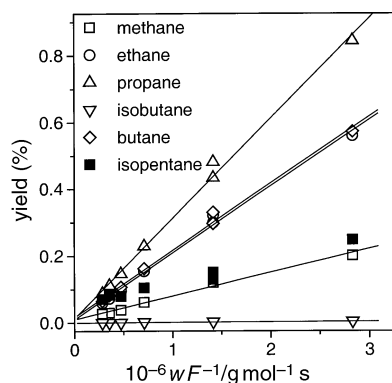


Fig. 5 Demonstration of differential conversion of *n*-pentane catalyzed by Pt₃W₂₀ at 473 K. Feed, *n*-pentane (1 kPa) with H₂ (50 kPa) in N₂ (50 kPa).

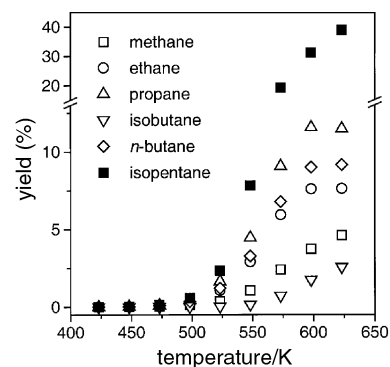


Fig. 6 Effect of temperature on conversion after 12 h TOS for reaction catalyzed by Pt_{0.3}W₂₀. Feed, *n*-pentane (1 kPa) with H₂ (50 kPa) in N₂ (50 kPa).

Pt_{0.3}W₁₀, Pt_{0.3}W₁₅, and Pt_{0.3}W₂₀ (Fig. 6). At temperatures higher than 623 K, deactivation was not negligible, and its onset correlated with the appearance of traces of unsaturated compounds in the product stream. Pt₁W₂₀ and Pt₃W₂₀ gave predominantly cracking products, with increasing concentrations of small saturated hydrocarbons at higher reaction temperatures. Trends in changes in yield and selectivity resulting from changes in the reaction temperature were found to be similar for *n*-pentane and for *n*-butane, with generally higher yields of cracking products observed with *n*-butane feeds.

Apparent activation energies (calculated from Arrhenius plots of reaction rates, estimated from nearly differential conversions, *e.g.*, Fig. 7) for *n*-pentane conversion are about the same (roughly 200 kJ mol⁻¹) for samples with different tungsten loadings (Table 6). An effect of an increase in tungsten loading was a slight reduction in the apparent activation energy for cracking and a slight increase in the apparent acti-

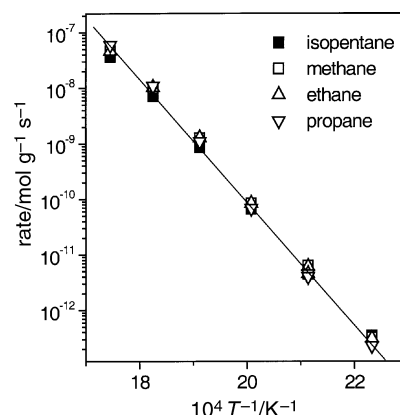


Fig. 7 Arrhenius plot: formation of products from *n*-pentane catalyzed by Pt_{0.3}W₂₀. Feed, *n*-pentane (1 kPa) with H₂ (50 kPa) in N₂ (50 kPa).

Table 5 Reaction rates for conversion of *n*-pentane at 473 K and of *n*-butane at 573 K, determined from differential conversions

Reactant	Catalyst composition (wt.%)		Rate of formation of product/mol (g of catalyst) ⁻¹ s ⁻¹					
	Pt	WO ₃	Methane	Ethane	Propane	Isobutane	<i>n</i> -Butane	Isopentane
<i>n</i> -pentane	0.3	10	1.21 × 10 ⁻⁸	2.26 × 10 ⁻⁸	3.73 × 10 ⁻⁸	0	3.77 × 10 ⁻⁹	1.45 × 10 ⁻⁸
	0.3	20	1.58 × 10 ⁻⁸	3.92 × 10 ⁻⁸	5.09 × 10 ⁻⁸	0	4.98 × 10 ⁻⁸	7.79 × 10 ⁻⁸
	3	20	7.07 × 10 ⁻⁸	2.00 × 10 ⁻⁷	3.00 × 10 ⁻⁷	1.26 × 10 ⁻⁹	2.00 × 10 ⁻⁷	6.74 × 10 ⁻⁸
<i>n</i> -butane	0.3	10	1.94 × 10 ⁻⁶	3.20 × 10 ⁻⁶	2.95 × 10 ⁻⁶	2.44 × 10 ⁻⁷		
	0.3	20	7.92 × 10 ⁻⁷	1.03 × 10 ⁻⁶	1.83 × 10 ⁻⁶	2.95 × 10 ⁻⁷		

Table 6 Apparent activation energies^a for conversion of *n*-butane and of *n*-pentane^b

Reactant	Catalyst composition (wt.%)		Apparent activation energy/kJ mol ⁻¹					
	Pt	WO ₃	Methane	Ethane	Propane	<i>n</i> -Butane	Isobutane	Isopentane
<i>n</i> -pentane	0.3	10	199	218	217	206	* ^c	179
	0.3	15	196	211	213	203	*	189
	0.3	20	180	196	204	198	*	204
	1	20	227	241	238	238	310	238
	3	20	254	272	267	248	298	300
<i>n</i> -butane	0.3	10	278	296	277	—	321	—
	0.3	20	233	295	288	—	301	—
	3	20	255	272	245	—	260	—

^a Standard deviation from linear fit, approximately 5 kJ mol⁻¹. ^b The feed partial pressures were the following: alkane, 1 kPa; H₂, 50 kPa; N₂, 50 kPa; data were determined from rates measured at temperatures in the range of 423–573 K; feed flow rate, 40 ml(NTP) min⁻¹; catalyst mass, 0.25 g. ^c * Conversion too low to allow determination.

vation energy for isomerization. Increasing the platinum content from 0.3 to 3 wt.% increased the apparent activation energies for both cracking (by *ca.* 60 kJ mol⁻¹) and isomerization (by *ca.* 100 kJ mol⁻¹). *n*-Butane conversion is characterized in general by higher apparent activation energies than *n*-pentane conversion, but the same trends relating the apparent activation energy and tungsten and platinum loading were observed for *n*-butane as for *n*-pentane, the only exception being that, for *n*-butane, high tungsten and platinum loadings correspond to reduced apparent activation energies for isomerization.

Whereas isomerization selectivities were found to decrease with increasing platinum loading, changes in tungsten loading (which is correlated with acidity) had only a little influence on catalyst performance. High cracking selectivities were generally related to the formation of small saturated hydrocarbons. These trends correlate with the generally higher apparent activation energies for isomerization reactions rather than for cracking reactions for catalysts with high platinum loadings. Catalysts with only 0.3% platinum, on the other hand, were characterized by lower apparent activation energies for isomerization rather than for cracking. These apparent activation energies account for the increase of cracking selectivity (especially for catalysts with high platinum contents) with increasing temperature, independent of the presence of H₂ in the feed.

Kinetics of reactions of *n*-pentane and of *n*-butane. Doubling the H₂ partial pressure from 40 to 80 kPa (total feed flow rate: 240 ml min⁻¹) with a hydrocarbon partial pressure of 0.17 kPa led to a halving of the total conversion, higher cracking selectivity, and a lower isomerization selectivity for both *n*-butane and *n*-pentane conversions. The increase in cracking

selectivity and the decrease in isomerization selectivity with increasing H₂ partial pressure were found to be greater for catalyst samples with high tungsten loadings (Table 7). Isomerization is favored at low H₂ partial pressures on catalysts with high tungsten loadings.

Reaction orders for a simple power law rate equation

$$r = kP_{\text{alkane}}^n P_{\text{H}_2}^m \quad (1)$$

were determined from the slopes of lines fitting rate *vs.* reactant partial pressure on logarithmic coordinates (Fig. 8). Measurements of the reaction orders in alkane (*n*) were made with H₂ partial pressures high enough to largely prevent catalyst deactivation.

Catalyst samples with high platinum loadings do not show a significant dependence of isomerization selectivity on H₂

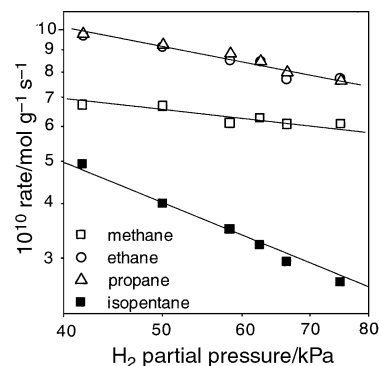


Fig. 8 Determination of orders of reaction in H₂. Data shown for various products of *n*-pentane conversion catalyzed by Pt_{0.3}W₂₀ at 573 K; data were determined for a partially deactivated catalyst.

Table 7 Effect of variation of H₂ partial pressure in the feed (at 41.7 or 75.0 kPa) on conversion of *n*-pentane at 523 K and of *n*-butane at 573 K^a

Reactant	Catalyst composition (wt.%)		Selectivity for isomerization (%)		10 ¹⁰ × isomerization rate /mol g ⁻¹ s ⁻¹		Total conversion (%)	
	Pt	WO ₃	41.7 kPa	75.0 kPa	41.7 kPa	75.0 kPa	41.7 kPa	75.0 kPa
<i>n</i> -pentane	0.3	10	9.1	7.2	5.0	4.2	1.60	0.91
	0.3	15	13.5	9.6	4.7	1.15	1.87	4.0
	0.3	20	24.2	16.6	5.4	4.5	4.90	2.65
<i>n</i> -butane	0.3	20	7.2	5.5	4.3	3.5	1.18	0.48
	3	20	0.9	1.1	42.2	15.6	1.70	1.10

^a The partial pressures of the other feed components were the following: alkane, 1 kPa; N₂, balance to give a total pressure of 101 kPa; feed flow rate, 120 ml(NTP) min⁻¹; catalyst mass, 0.25 g.

partial pressure. Increasing *n*-pentane partial pressures in the range of 1 to 5 kPa reduced total conversion and increased isomerization selectivity (Table 8). These effects are strongest for catalysts with high tungsten loadings. Reaction orders (*n* and *m*) for cracking products of *n*-pentane are in the range of -0.4 ± 0.2 and do not vary significantly with tungsten and platinum loadings. Reaction orders in H₂ (*m*) for isomerization are -0.9 ± 0.2 and in alkane (*n*) are -0.1 ± 0.2 . The latter values are more negative for butane (< -1).

Discussion

Comparison of performance of WO_x/TiO₂ and related alkane isomerization catalysts

The data confirm that WO_x/TiO₂ (WTi) is catalytically active for alkane isomerization, but its activity is markedly lower than that of sulfated zirconia, some form of which is active enough to have found application as a commercial catalyst for isomerization of C₅ and C₆ alkanes.¹ For example, WTi catalyzes *n*-pentane isomerization measurably at 573 K, whereas sulfated zirconia catalyzes this reaction measurably at temperatures as low as about 320 K.²⁰

The activity and selectivity of WTi for isomerization are similar to those of tungstated zirconia (WZr) (Table 9), but WTi catalysts are different from WZr in producing much higher yields of alkenes, and, likely as a consequence of the presence of the alkenes, they are deactivated more rapidly than WZr. For example, deactivation of WTi is too fast to allow detection of isomerization activity at 523 K with the reactant in the presence of N₂ alone, whereas deactivation of WZr at 523 K begins after an induction period at 1.5 h on stream. However, the addition of H₂ to the feed suppresses alkene formation catalyzed by WTi and allows measurement of some isomerization activity. Addition of platinum to WTi improves its performance for alkane isomerization, much as it improves the performance of WZr for this reaction.

Because WTi is not nearly as active an alkane isomerization catalyst as sulfated zirconia and not nearly as selective an alkane isomerization catalyst as WZr, it is not expected to be practically useful for this reaction.

Bifunctional catalysis by platinum-containing WTi

Characteristics of the performance of the PtW catalyst, including its rapid deactivation (presumably by coke formation) at

Table 8 Effect of variation of alkane partial pressure (at 0.9 or 5.3 kPa) in conversion of *n*-pentane (at 523 K) and of *n*-butane (at 573 K)

Reactant	Catalyst composition (wt.%)		Selectivity for isomerization (%)		10 ¹⁰ × isomerization rate /mol g ⁻¹ s ⁻¹		Total conversion (%)	
	Pt	WO ₃	0.9 kPa	5.3 kPa	0.9 kPa	5.3 kPa	0.9 kPa	5.3 kPa
<i>n</i> -pentane	0.3	10	8.9	12.8	1.03	2.00	4.9	2.0
	0.3	15	11.5	17.2	1.98	1.31	6.9	2.2
	0.3	20	18.5	36.3	3.62	4.15	7.5	2.3
<i>n</i> -butane	0.3	10	3.0	3.9	1.20	0.72	9.5	3.4
	0.3	20	6.1	8.0	0.99	0.53	6.8	1.8
	3	20	1.0	0.7	4.30	7.39	35.1	22.4

Table 9 *n*-Pentane isomerization in the presence of various catalysts

Catalyst ^a	Temperature /K	WHSV/g of alkane/(g of catalyst × h)	Reactant partial pressures/kPa	Notes	Total <i>n</i> -pentane conversion rate/mol g ⁻¹ s ⁻¹	Total <i>n</i> -pentane conversion (%)	Approx. isomerization selectivity (%)	Reference
W ₂₀ Ti T _c = 923 K	573	0.072	<i>n</i> -pentane: 1 N ₂ : 50 H ₂ : 50	very slow deactivation	8.4 × 10 ⁻⁹	3	75	this work
W ₂₀ Ti T _c = 923 K	523	0.072	<i>n</i> -pentane: 1 N ₂ : 100	no activity observed at temperatures up to 673 K, deactivation too fast	0	0	—	this work
W ₁₉ Zr T _c = 923 K	523	0.072	<i>n</i> -pentane: 1 N ₂ : 100	rapid deactivation	1.1 × 10 ⁻⁹	0.8	80	23
Pt _{0.3} W ₂₀ Ti	523	0.18	<i>n</i> -pentane: 1 N ₂ : 50 H ₂ : 50	nearly constant activity	1.5 × 10 ⁻⁸	2.1	35	this work
Pt _{0.3} W ₁₉ Zr	523	0.036	<i>n</i> -pentane: 2 N ₂ : 50 H ₂ : 50	induction period followed by deactivation	2 × 10 ⁻⁸	7.1	95	this work
Pt _{0.3} S _{1.8} Zr	479	0.347	<i>n</i> -pentane: 7.2 H ₂ : 223 He: 869.8	nearly constant activity	6.7 × 10 ⁻⁷	24.8	92	16
Pt _{0.3} Al	645	0.19	<i>n</i> -pentane: 460 H ₂ : 640	standard naphtha reforming catalyst	1.3 × 10 ⁻⁷	17.9	94	24

^a Note: T_c is calcination temperature.

low H_2 partial pressures and high temperatures, its increasingly high cracking selectivity at increasing temperatures, and the suppression of its deactivation in the presence of high H_2 partial pressures, are typical of the performance of bifunctional catalysts of the type used for naphtha reforming,²¹ exemplified by platinum supported on chlorided Al_2O_3 . The classical bifunctional catalysts activate an alkane by first dehydrogenating it (*e.g.*, on Pt), and the resultant alkene is transferred to an acidic site on the Al_2O_3 (which is made a stronger proton donor by the presence of chloride), where it is protonated to give a carbenium ion, which isomerizes. The isomerized carbenium ion gives a proton back to the catalyst to form an alkene, which is transferred to a hydrogenation site to form the product alkane.²¹ Alternatively, the carbenium ion intermediate can undergo β -scission (cracking) or be involved in C–C bond formation reactions.²²

The unsaturated intermediates are responsible for the loss of isomerization activity, *e.g.*, by formation of higher-molecular-weight species, including coke, which blocks catalytic sites. Platinum in such catalysts, including ours, helps to minimize deactivation resulting from coke formation by catalyzing hydrogenation of unsaturated species that are coke precursors.

In our PtW/Ti samples, the platinum dispersions were about the same for the catalysts containing 0.3 and 3% Pt, and thus there was a much higher platinum surface area in the latter. Consequently, a longer time was required to cover the platinum sites (with coke or related deposits), and thus a longer time was required to suppress the dehydrogenation function of the catalyst containing 3% Pt.

The fact that the dehydrogenation function remained active over the whole period of operation is demonstrated by the data showing that at long times on stream exclusively unsaturated products were observed in the product stream. Under these conditions the catalysts were still active for dehydrogenation, but the acidic sites had been rendered largely inactive for isomerization, evidently having undergone faster deactivation than the platinum dehydrogenation sites. We infer that at short times on stream, when almost no unsaturated products desorbed from the catalyst surfaces, the acidic sites effectively removed almost all the alkenes formed on the platinum sites. The data show that the catalyst performance, including the kinetics, was nearly independent of the differences in acid strength from one sample to another, which correlates with the tungsten loading (Table 2).

By inference from this observation, we might speculate that the differences in catalytic performance between tungstated zirconia and tungstated titania are largely unrelated to differences between the acid strengths of the zirconia and titania supports. Thus, we speculate instead that the differences are related primarily to the role of platinum, perhaps influenced by the structures of platinum and/or platinum's role in spillover of hydrogen. Data are lacking to provide insight into these issues.

The occurrence of a bifunctional reaction network involving acid- and metal-catalyzed reactions is supported by the observed reaction kinetics characterizing partially deactivated catalysts. Reaction orders in H_2 for *n*-butane and *n*-pentane conversion catalyzed by PtW/Ti are negative (roughly -1), as has been observed before for this kind of network.¹⁹ Because

the kinetics was not influenced significantly by the acidity of the catalysts and because the unsaturated intermediates play an important role in the chemistry, we infer that the dehydrogenation (metal) function was more important in influencing the catalyst performance than the acidic function—but we are aware of the impreciseness of this statement.

As the reaction network is complex and the primary and secondary reactions not resolved, the kinetics results cannot be regarded as more than just empirical; they represent overall reactions and not a resolution of the individual reactions.

Acknowledgements

The work done in Munich was supported financially by the Deutsche Forschungsgemeinschaft (SFB 338). The cooperation with the University of California, Davis, was supported by the Alexander von Humboldt-Stiftung and the BMBF (Max Planck-Research Award to HK). BCG thanks the Alexander von Humboldt-Stiftung for support in Munich.

References

- 1 C. Gosling, R. Rosin, P. Bullen, T. Shimizu and T. Imai, *Petrol. Technol. Q.*, 1997/98, Winter, 55.
- 2 J. C. Yori, J. C. Lui and J. M. Parera, *Catal. Today*, 1989, **5**, 493.
- 3 F. T. T. Ng and N. Horvat, *Appl. Catal. A*, 1995, **123**, 195.
- 4 E. Ebitani, J. Konishi and H. Hattori, *J. Catal.*, 1991, **130**, 257.
- 5 G. Larsen and L. M. Petkovic, *Appl. Catal. A*, 1996, **148**, 155.
- 6 S. R. Vaudagna, R. A. Comelli and N. S. Figoli, *Appl. Catal. A*, 1997, **164**, 265.
- 7 F. Garin, D. Andriamasinoro, A. Abdulsamad and J. Sommer, *J. Catal.*, 1991, **131**, 199.
- 8 K. Tanabe, H. Hattori and T. Yamaguchi, *Crit. Rev. Surf. Chem.*, 1999, **1**, 1.
- 9 M. Hino and K. Arata, *Chem. Lett.*, 1979, 1259.
- 10 M. Scheithauer, T.-K. Cheung, R. E. Jentoft, R. K. Grasselli, B. C. Gates and H. Knözinger, *J. Catal.*, 1998, **180**, 1.
- 11 G. Kunzmann, Doctoral Dissertation, Universität München, 1987.
- 12 T.-K. Cheung, J. L. d'Itri and B. C. Gates, *J. Catal.*, 1995, **151**, 464.
- 13 G. C. Bond, S. Flamerz and L. Van Wijk, *Catal. Today*, 1987, **1**, 229.
- 14 E. Iglesia, D. G. Barton, S. L. Soled, S. Miseo, J. E. Baumgartner, W. E. Gates, G. A. Fuentes and G. D. Meitzner, *Stud. Surf. Sci. Catal.*, 1996, **101**, 533.
- 15 D. C. Vermaire and P. C. van Berge, *J. Catal.*, 1989, **116**, 309.
- 16 J. A. Anderson, F. K. Chong and C. H. Rochester, *J. Mol. Catal. A: Chem.*, 1999, **140**, 65.
- 17 S. Eibl, Doctoral Dissertation, Universität München, 1999.
- 18 H. Knözinger, in *Proc. Int. Symp. Acid-Base Catalysis, Sapporo*, ed. K. Tanabe, H. Hattori, T. Yamaguchi and T. Tanaka, Elsevier, Amsterdam, 1988, p. 147.
- 19 G. F. Froment and K. B. Bischoff, *Chemical Reactor Analysis and Design*, Wiley, New York, 2nd edn., 1989, p. 93.
- 20 K. Arata, *Adv. Catal.*, 1990, **37**, 165.
- 21 B. C. Gates, J. R. Katzer and G. C. A. Schuit, *Chemistry of Catalytic Processes*, McGraw-Hill, New York, 1979, p. 190.
- 22 F. C. Jentoft and B. C. Gates, *Top. Catal.*, 1997, **4**, 1.
- 23 G. Larsen, E. Lotero, S. Raghavan, R. D. Parra and C. A. Querini, *Appl. Catal. A*, 1996, **139**, 201.
- 24 J. H. Sinfelt, H. Hurwitz and J. C. Rohrer, *J. Catal.*, 1962, **1**, 481.